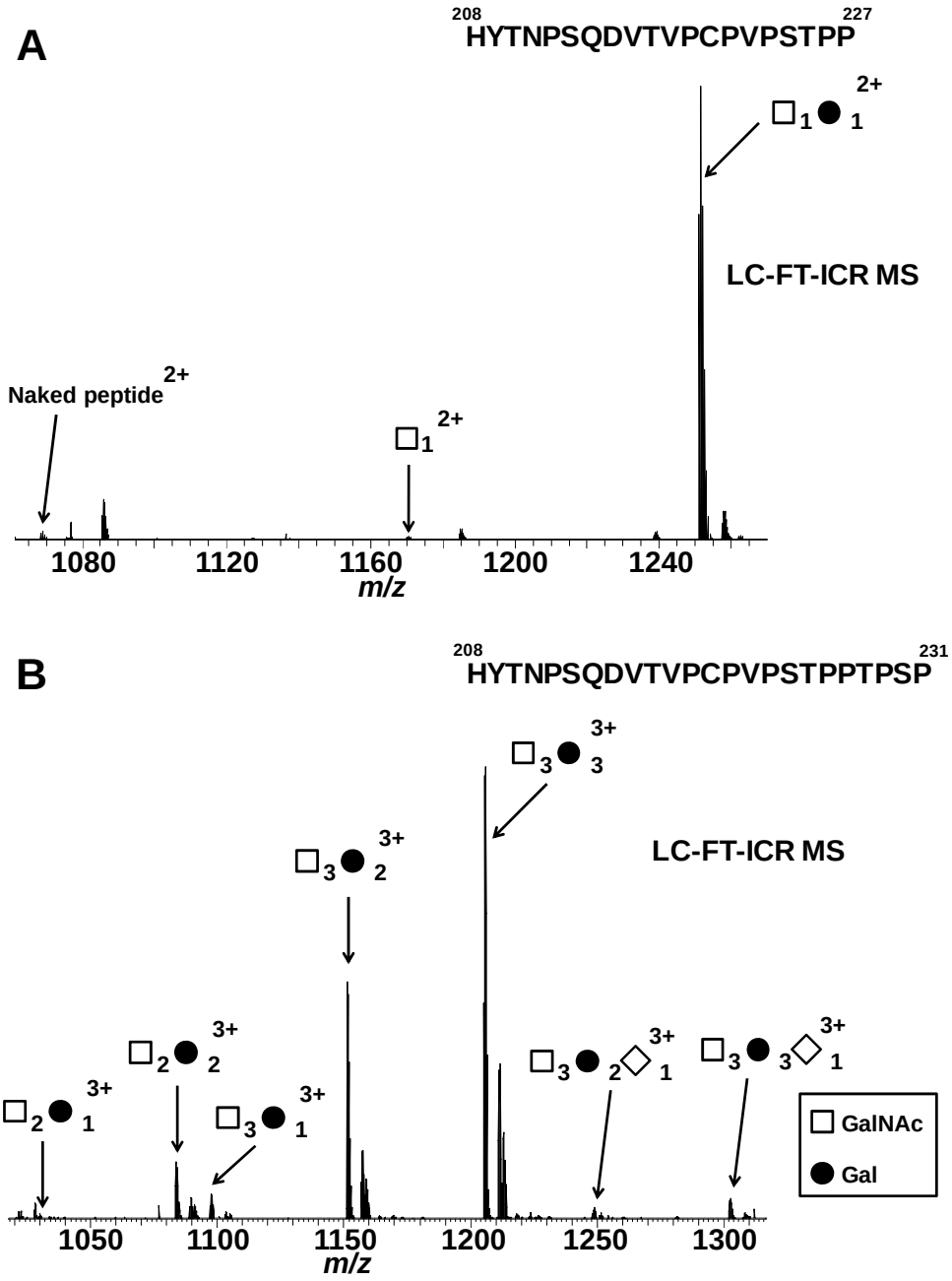

Supplemental Figure 1. IgA-specific protease+trypsin-released N-terminal fragments of IgA1 HR *O*-glycopeptides. IgA1 HR N-terminal glycopeptides released by IgA-specific protease TIGR4 and trypsin (**a**, H208-P227) and HK50 and trypsin (**b**, H208-P231). The H208-227 fragment was observed as three different ion species, including one with no modification (naked peptide), another with a single GalNAc, and the dominant species with a GalNAc-Gal disaccharide. These observed IgA1 HR *O*-glycopeptides included a few that were Gal-deficient or without glycosylation at T225. The H208-P231 fragment further corroborated this conclusion. All identified N-terminal fragments are listed in supplemental **Table 1**.

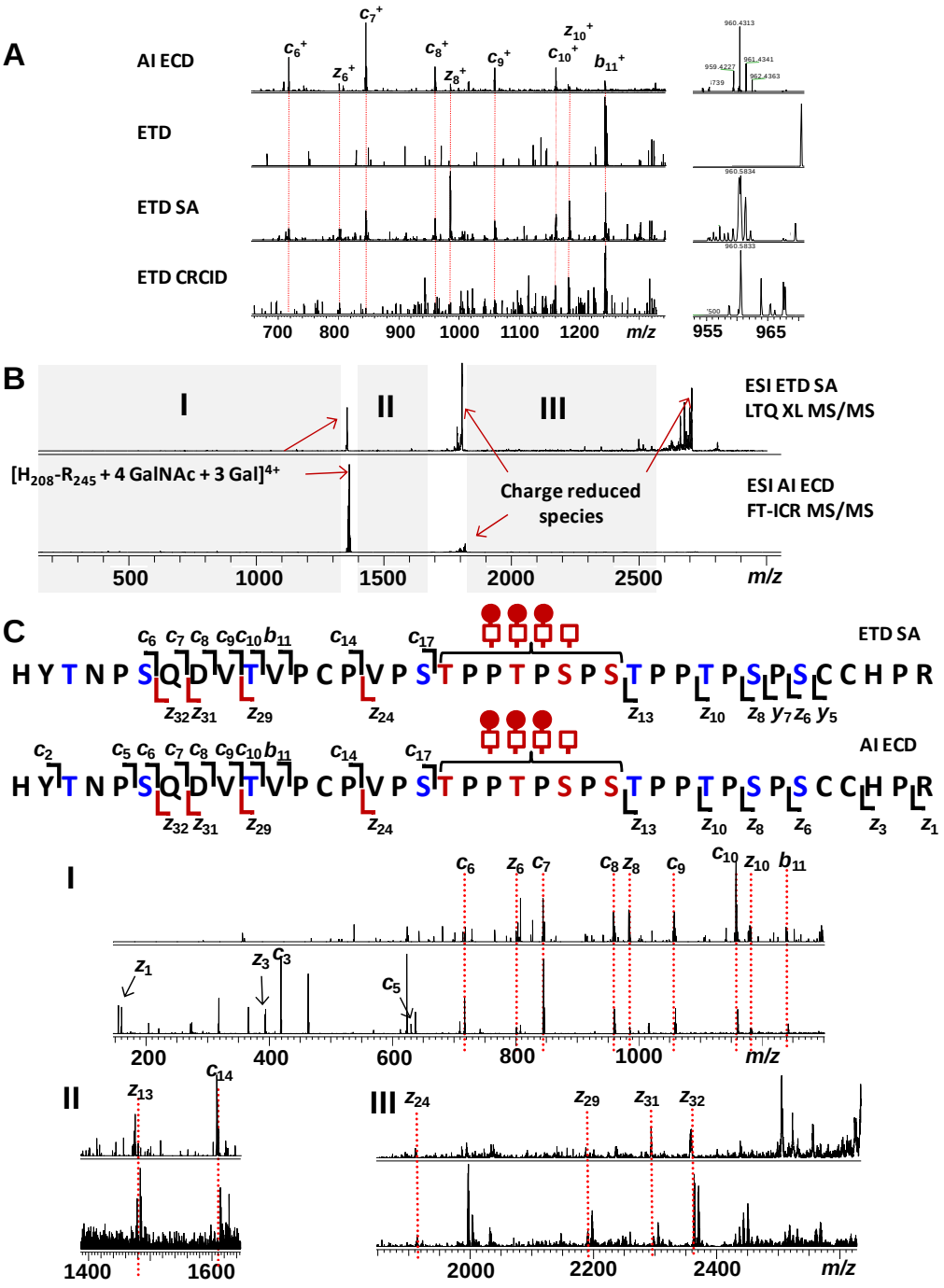

ESI AI ECD FT-ICR MS/MS Fragments observed

m/z	charge	assignment
317.14	1	c2
393.21	1	z3
630.30	1	c5
717.33	1	c6
801.32	1	*z6+1*
845.40	1	*c7*
960.43	1	*c8-1*
985.51	1	z8+1
1058.49	1	*c9-1*
1159.54	1	c10-1
1181.50	1	*z10-1*
1242.60	1	b11
1359.61	4	M + □4●3
1478.68	1	z13+1
1613.77	1	c14
1896.85	1	c17
1912.88	2	z24+1 + □4●3
2190.02	2	z29+1 + □4●3
2297.10	2	z31+1 + □4●3
2560.71	2	z32+1 + □4●3

ESI ETD SA LTQ XL MS/MS Fragments observed

m/z	charge	assignment
717.4	1	c6
800.8	1	*z6*
960.7	1	*c7*
959.9	1	*c8-1*
984.3	1	z8
1057.2	1	*c9-1*
1158.6	1	c10-1
1180.1	1	*z10-2*
1242.1	1	b11
1360	4	M + □4●3
1478	1	z13+1
1613	1	c14
1896	1	c17
1912	2	z24 + □4●3
2189	2	z29 + □4●3
2296	2	z31 + □4●3
2561	2	z32 + □4●3

Supplemental Figure 2. Comparison of AI-ECD and ETD SA fragmentation of IgA1 HR. Results of preliminary experiments with direct infusion Nanomate ESI ETD SA LTQ XL MS/MS of the IgA1 HR [H208-R245 + 4 GalNAc + 3 Gal]$^{4+}$ trypsin-generated fragment were compared with those using AI-ECD FT-ICR MS/MS of the same ion species. In a fashion similar to that with our previous ECD analysis of IgA1 HR *O*-glycopeptides, no *c* or *z* fragment was observed with ETD alone. When supplemental activation (SA) was included, several *c*, *z*, and *b* fragments were generated (**a**). The ETD spectra appear to have a greater conversion of precursor ion into charge-reduced species in the overall spectrum (**b**). Upon closer examination (**c**), the ETD SA fragments were no better for localizing individual sites of *O*-glycosylation in the clustered region than were the AI-ECD-generated fragments, suggesting that the mechanisms of dissociation were essentially identical.

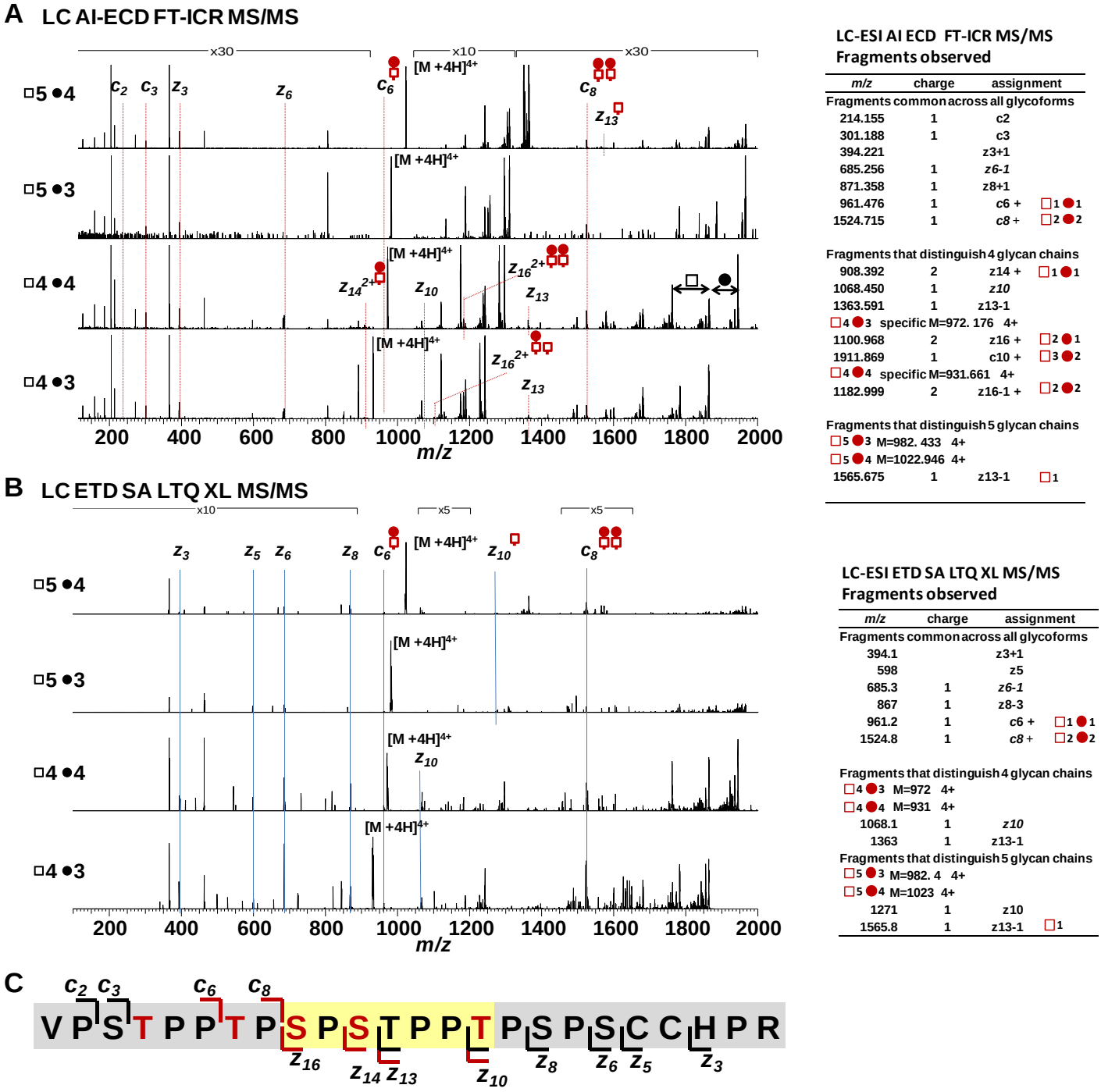

LC-ESI AI ECD FT-ICR MS/MS Fragments observed

m/z	charge	assignment	
Fragments common across all glycoforms			
214.155	1	c2	
301.188	1	c3	
394.221		z3+1	
685.256	1	*z6-1*	
871.358	1	z8+1	
961.476	1	c6 +	□1 ●1
1524.715	1	*c8* +	□2 ●2
Fragments that distinguish 4 glycan chains			
908.392	2	z14 +	□1 ●1
1068.450	1	*z10*	
1363.591	1	z13-1	
□4 ●3 specific M=972. 176 4+			
1100.968	2	z16 +	□2 ●1
1911.869	1	c10 +	□3 ●2
□4 ●4 specific M=931.661 4+			
1182.999	2	z16-1 +	□2 ●2
Fragments that distinguish 5 glycan chains			
□5 ●3 M=982. 433 4+			
□5 ●4 M=1022.946 4+			
1565.675	1	z13-1	□1

LC-ESI ETD SA LTQ XL MS/MS Fragments observed

m/z	charge	assignment	
Fragments common across all glycoforms			
394.1		z3+1	
598		z5	
685.3	1	*z6-1*	
867	1	z8-3	
961.2	1	c6 +	□1 ●1
1524.8	1	*c8* +	□2 ●2
Fragments that distinguish 4 glycan chains			
□4 ●3 M=972 4+			
□4 ●4 M=931 4+			
1068.1	1	*z10*	
1363	1	z13-1	
Fragments that distinguish 5 glycan chains			
□5 ●3 M=982. 4 4+			
□5 ●4 M=1023 4+			
1271	1	z10	
1565.8	1	z13-1	□1

Supplemental Figure 3. Data-dependent LC-ECD/ETD analysis of IgA1 HR *O*-glycopeptides. A. LC-AI-ECD MS/MS (**a**) and LC-ETD SA MS/MS (**b**) of four most abundant IgA1 HR V222-R245 *O*-glycoforms isolated and fragmented within a single LC-MS analysis by each instrument. The ECD/ETD fragments that all four IgA1 HR *O*-glycoforms share in common were readily identified in all spectra with c_6 and c_8 ions. With these spectra, a GalNAc-Gal disaccharide can be assigned to T225 and T228. The z_{10} fragment that distinguished the glycoforms with four *O*-glycan chains from those with five is also readily apparent. Fragments between S230 and P234 were less abundant, but still distinguishable, in the LC AI-ECD MS/MS analysis by accurate mass (**c**). Each individual fragmentation spectrum represents the sum of 6-8 scans. This number is considerably less than the 100 scans required for off-line preparations and allows analysis of clinically practical amounts of IgA1. All isolated precursor ions were quadruply charged.

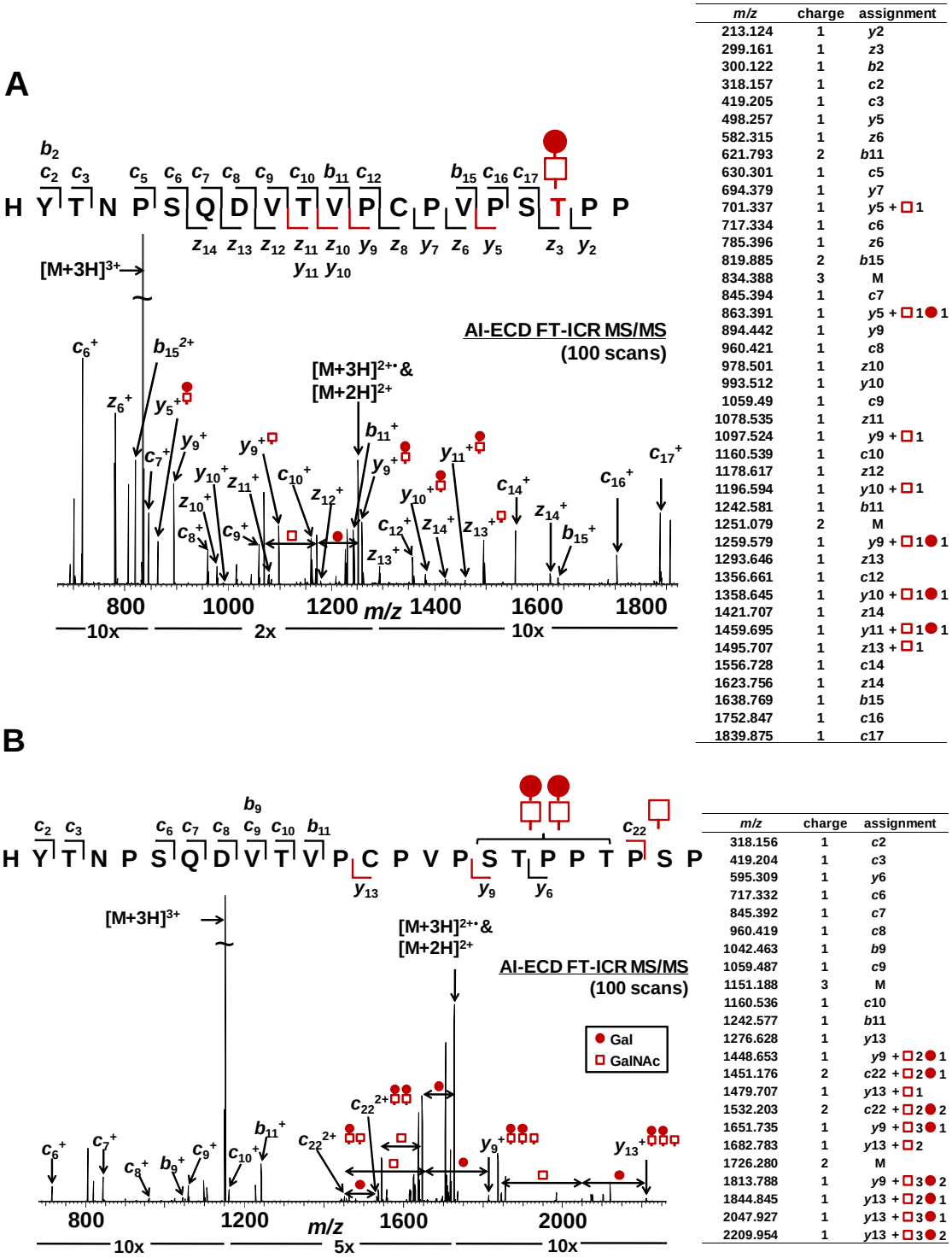

m/z	charge	assignment
213.124	1	*y*2
299.161	1	*z*3
300.122	1	*b*2
318.157	1	*c*2
419.205	1	*c*3
498.257	1	*y*5
582.315	1	*z*6
621.793	2	*b*11
630.301	1	*c*5
694.379	1	*y*7
701.337	1	*y*5 + □1
717.334	1	*c*6
785.396	1	*z*6
819.885	2	*b*15
834.388	3	M
845.394	1	*c*7
863.391	1	*y*5 + □1●1
894.442	1	*y*9
960.421	1	*c*8
978.501	1	*z*10
993.512	1	*y*10
1059.49	1	*c*9
1078.535	1	*z*11
1097.524	1	*y*9 + □1
1160.539	1	*c*10
1178.617	1	*z*12
1196.594	1	*y*10 + □1
1242.581	1	*b*11
1251.079	2	M
1259.579	1	*y*9 + □1●1
1293.646	1	*z*13
1356.661	1	*c*12
1358.645	1	*y*10 + □1●1
1421.707	1	*z*14
1459.695	1	*y*11 + □1●1
1495.707	1	*z*13 + □1
1556.728	1	*c*14
1623.756	1	*z*14
1638.769	1	*b*15
1752.847	1	*c*16
1839.875	1	*c*17

m/z	charge	assignment
318.156	1	*c*2
419.204	1	*c*3
595.309	1	*y*6
717.332	1	*c*6
845.392	1	*c*7
960.419	1	*c*8
1042.463	1	*b*9
1059.487	1	*c*9
1151.188	3	M
1160.536	1	*c*10
1242.577	1	*b*11
1276.628	1	*y*13
1448.653	1	*y*9 + □2●1
1451.176	2	*c*22 + □2●1
1479.707	1	*y*13 + □1
1532.203	2	*c*22 + □2●2
1651.735	1	*y*9 + □3●1
1682.783	1	*y*13 + □2
1726.280	2	M
1813.788	1	*y*9 + □3●2
1844.845	1	*y*13 + □2●1
2047.927	1	*y*13 + □3●1
2209.954	1	*y*13 + □3●2

Supplemental Figure 4. AI-ECD of N-terminal IgA1 HR fragments. Direct infusion Nanomate ESI AI-ECD FT ICR MS/MS of IgA1 HR protease-trypsin N-terminal fragments H208-P227 and H208-231. A single GalNAc-Gal disaccharide was localized to T225 for the dominant H208-P227 fragment (see Supplementary Fig. 1A). Still, there are several *z* and *y* fragments from the C-terminal end of this peptide that corresponded to the loss of the disaccharide (below the sequence in black), rendering the assignment ambiguous. The same feature was found for the H208-P231 + 3 GalNAc + 2 Gal fragment with a y_6 ion lacking a carbohydrate residue. The ambiguity of these AI-ECD spectra contrasts to the clarity for the spectra of the C-terminal fragments that include a C-terminal arginine with loss of carbohydrate residues from the parent ion species but no ambiguity in the *c*, *z*, and *y* fragments in the spectra for assignment of the sites of *O*-glycosylation.